Results in Engineering 28 (2025) 107590

Contents lists available at ScienceDirect

Results in Engineering

journal homepage: www.sciencedirect.com/journal/results-in-engineering

Research paper

Quantitative evaluation of surface material effects on particle impact damper performance- a time domain analysis

Muhammad Ayaz Akbar [a,b], Hassan Raza [c,*], Naveed Husnain [d]

[a] Institute of Advanced Interdisciplinary Technology, Shenzhen MSU-BIT University, Shenzhen, China
[b] Department of Material Science, Beijing Institute of Technology, Beijing, China
[c] Department of Mechanical Engineering, Hong Kong Polytechnic University, China
[d] Department of Mechanical Engineering, Faculty of Engineering and Technology, Bahauddin Zakariya University Multan 60800, Pakistan

ARTICLE INFO

Keywords:
Passive vibration control
Structural dynamics
Particle impact dampers
Coefficient of restitution
Impact

ABSTRACT

Although particle impact dampers (PIDs) have received much attention for their effectiveness in passive vibration reduction, the influence of impact surface material on damping performance, especially in the time-domain, remains inadequately investigated. This study examines the impact of six materials; three hard (Aluminium, Steel, Acrylic) and three soft (Rubber, Polyethylene foam, Polyurethane foam), on vibration attenuation utilizing a single-degree-of-freedom system. A verified numerical model that includes the coefficient of restitution (COR) is utilized in conjunction with experimental testing. The findings indicate that Polyurethane foam (COR = 0.36) exhibits superior damping efficacy, diminishing vibration amplitude by 52.16% and impact force by 78% in comparison to Aluminium (COR = 0.82). Rubber and PE foam provide decreases of 21.38% and 22.35%, respectively, whilst hard surfaces demonstrate negligible enhancement. The numerical model strongly correlates with experimental data, with a maximum variation of 7.14%. These findings indicate that soft, energy-absorbing materials markedly improve PID performance, providing enhanced vibration attenuation and less structural stress. The research offers a pragmatic paradigm for enhancing PID design in applications necessitating elevated damping efficiency, mechanical safety, and minimal operational noise.

Nomenclature

Symbols	Description
$\ddot{\mathbf{x}}$	Acceleration of primary structure; m/s^2
$\ddot{\mathbf{y}}$	Acceleration of particle; m/s^2
d	Clearance; *m*
e	Coefficient of restitution;
c	Damping coefficient; Ns/m
y	Displacement of particle; m
x	Displacement of primary structure; m
F(**t**)	Excitation force; N
$\mathbf{x}_0$	Initial position of primary structure; m
$\mathbf{y}_0$	Initial position of particle; m
$\dot{\mathbf{x}}_0$	Initial velocity of primary structure; m/s
$\dot{\mathbf{y}}_0$	Initial velocity of particle; m/s
M	Mass of primary structure; kg
m	Mass of the particle; kg
k	Spring constant; *N/m*
$\dot{\mathbf{y}}$	Velocity of particle; *m/s*
$\dot{\mathbf{x}}$	Velocity of primary structure; *m/s*
$\dot{\mathbf{y}}_\mathbf{n}^+$	Velocity of particle after nth impact; *m/s*
$\dot{\mathbf{y}}_\mathbf{n}^-$	Velocity of particle before nth impact; *m/s*
$\dot{\mathbf{x}}_\mathbf{n}^+$	Velocity of primary structure after nth impact; *m/s*
$\dot{\mathbf{x}}_\mathbf{n}^-$	Velocity of primary structure before nth impact; *m/s*
Greek Symbols	
ω	Frequency of excitation force; rad/s
$\omega_\mathbf{n}$	Natural frequency of primary structure; rad/s
μ	Mass ratio; m/M
η	Reduction effect
Abbreviations	
PID	Particle impact damper
RMS	Root Mean Square
PE	Polyethylene
PU	Polyurethane
COR	Coefficient of Restitution
FFT	Fast Fourier Transformation

* Corresponding author.
E-mail addresses: mayazakbar@smbu.edu.cn (M.A. Akbar), Hraza@polyu.edu.hk (H. Raza), naveedhusnain@bzu.edu.pk (N. Husnain).

https://doi.org/10.1016/j.rineng.2025.107590
Received 31 July 2025; Received in revised form 30 September 2025; Accepted 5 October 2025
Available online 6 October 2025

1. Introduction

Vibration control is a critical in many engineering applications, including civil, mechanical, and aerospace structures, where excessive oscillations can compromise safety, performance, and service life. Various passive, semi-active, and active control methods have been developed to mitigate vibrations, each with advantages and limitations [1–5]. Among these, particle impact dampers (PIDs) have attracted attention due to their simplicity, robustness, and effectiveness in dissipating energy through inelastic collisions, making them a promising solution for structural vibration suppression. PID consists of a container filled with single or multiple particles. The principle of damping is based on the particle-particle and particle-wall impacts. The impacts and friction between particles and walls of the container result in energy dissipation and momentum exchange leading to the damping of the vibrations of the primary structure [6–8]. In addition, the particle impact damper possesses various advantages over other passive vibration attenuation devices [9]. Particle impact dampers require a simple installation, are not sensitive to the direction of excitation, and can work in harsh conditions where other devices cannot be installed [10,11]. The particle damper is not noticeably sensitive to oil contamination and can attenuate vibrations under various types of excitations [12]. Additionally, PID can be considered a simple, reliable, and affordable device for vibration control applications [13,14]. The particle impact damper can function in multiple directions and over a wide range of excitation frequencies [15,16].

Considering the potential of the particle impact dampers, optimization and design guidelines become highly important in this research area. Nonlinear nature of PID, the development of analytical, numerical, and even experimental methodologies for performance optimization of PID is highly difficult [17–20]. Various researchers [21–24] have reported methods and techniques to design a particle impact damper for improved vibration attenuation, leading to contradicting opinions about the design guidelines [25,26]. Most of the available guidelines or design methodologies are based on specific applications or trial and error [27–31]. The literature resolves that the clearance, coefficient of restitution, and mass ratio are the highly influential design parameters [32–34]. However, the studies are limited to specific cases or application. It is understood that an optimum combination of these parameters can provide an optimum design of particle impact damper. However, determining the optimum combination is highly complicated due to the highly nonlinear relationship of these parameters with the excitation [35–39]. There are fundamental design guideline developed from the efforts of the scholars, such as the optimum clearance magnitude and the mass ratio [40–42].

The optimum parameters selection require an understanding of the excitation force [43]. It is shown by researchers that the performance of a particle damper is independent of the particle-particle interactions [44]. It is also shown that the model using singular particles has similar results to the model with multiple particles. Although, the optimum design parameters can still be determined for a specific excitation force [45]. Optimum clearance depends on the excitation force, and the mass ratio is selected by the factor that how much extra mass can be added to the primary structure [46–49]. It is proved by a few researchers that a single-particle damper can be the better choice but the intense impact with a single heavy mass may raise questions about the safety of the primary structure [50]. Such a problem has led researchers to propose multi-particle dampers to generate multiple less intense impacts to protect the primary structure [51–56]. The multi-particle impact damper can protect the structure during operation but at a cost of relatively lower damping with higher functional noise.

Particle impact dampers (PIDs) have been widely studied for their effectiveness in vibration attenuation, with most research focusing on parameters such as particle size, mass ratio, and enclosure geometry. However, relatively few studies have examined the influence of impact surface properties on PID performance [57] investigated the role of surface material properties and found that metallic particles exhibited superior damping performance compared to other materials. This suggests that softer particles may be less effective in reducing structural vibrations. More recently, [58] explored the effects of soft and hard impact conditions in single-particle impact dampers within the frequency domain. Their study provided an optimal design strategy based on numerical and experimental analysis by incorporating the viscoelastic behavior of soft materials. Building upon these studies, this research extends the evaluation of PID performance by investigating the role of different cushioning materials in a time-domain analysis. The performance of PIDs is strongly influenced by the coefficient of restitution of the impact materials, which governs the energy dissipation during inelastic collisions [59]. Recent studies have shown that selecting materials with appropriate restitution properties can significantly enhance damping efficiency and reduce structural vibration [60–63]. Understanding the relationship between material properties, impact dynamics, and energy dissipation is therefore critical for effective damper design [64–67]. Specifically, this study compares the effects of soft impact materials (Rubber, Polyethylene (PE) foam, and Polyurethane (PU) foam) with traditional hard impact surfaces. A simplified numerical model incorporating the coefficient of restitution (COR) of different materials is developed and validated through experiments. Additionally, the structural response under resonant excitation is analyzed to determine the effectiveness of various impact surfaces in vibration attenuation. By considering the nature of the impact, this study provides insights into optimizing PID design while maintaining structural integrity and minimizing operational noise, offering a practical and cost-effective solution for enhanced damping performance.

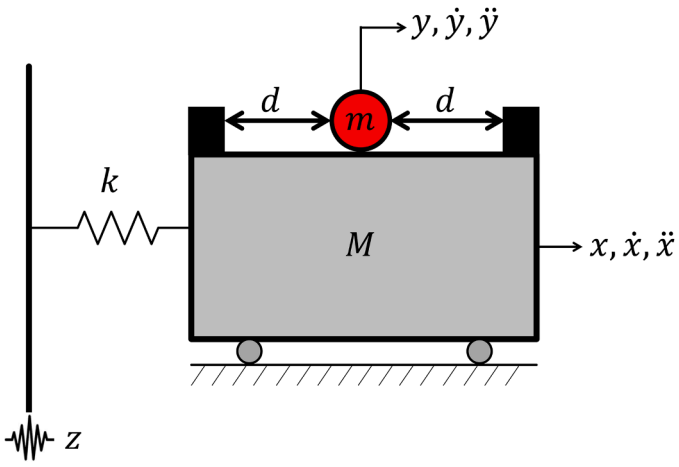

Fig. 1. A mechanical model of the SDOF structure equipped with a particle impact damper.

2. Theory

Considering the challenges and nonlinear relationships with the contact force model, a mechanical model with a coefficient of restitution is used to simplify the simulations of particle impact dampers. The coefficient of restitution can be sufficient to model the collision surface in PID. This model utilizes the coefficient of restitution of the impact surface to determine the energy dissipation at each impact.

A general model of the single-degree-of-freedom system with a particle impact damper is presented in Fig. 1. Compared with the previous model, the nonlinear components of the contact are removed in this model. The equation of motion of the primary structure and particle is written as,

$$M\ddot{x} + k(x - z) = 0 \tag{1}$$

$$m\ddot{y} = 0 \tag{2}$$

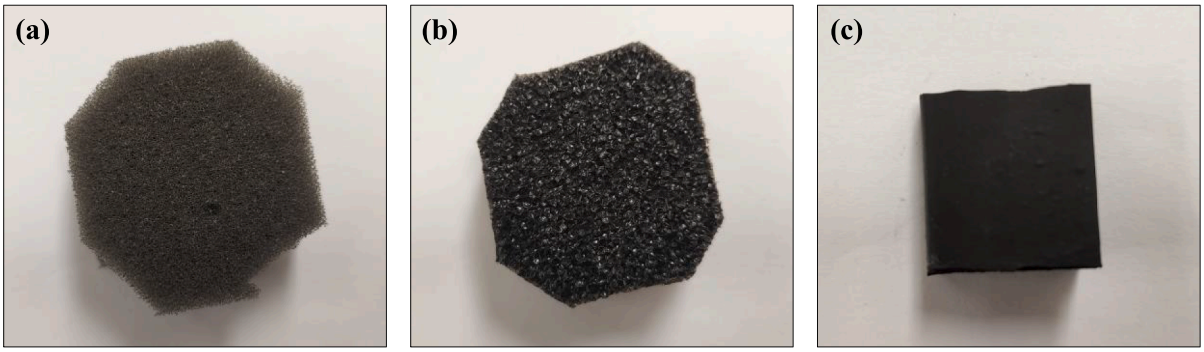

Fig. 2. Materials used in the experiments **(a)** Polyurethane (PU) foam **(b)** Polyethylene (PE) foam **(c)** Rubber.

Here M, k, x, $\dot{x}$, $\ddot{x}$ represents the mass, stiffness, displacement, velocity, and acceleration of primary structure, while m, y,$\dot{y}$, $\ddot{y}$ represents the mass, displacement, velocity, and acceleration of particle respectively. It is worth noting that Eqs. (1) and (2) describe the equations of motion of two independent masses (the primary structure and the particle), assuming that neither internal damping nor frictional effects influence their motion. In this baseline representation, the attenuation of vibration in the primary structure arises only from inelastic collisions, where momentum transfer and energy dissipation during impact produce the effective damping. Therefore, the impact is modelled with conservation of momentum and coefficient of restitution. The COR-based model was adopted for its simplicity and practicality, as it directly represents the energy absorption capability of the impact surface. Moreover, the coefficient of restitution (e) represents the amount of energy dissipated at each impact. The velocities of the primary structure and particle change at each impact, and the velocities after the impacts are determined by using conservation of momentum and coefficient of restitution at each impact. The accurate calculation of change in velocity at each impact depends on change in momentum and coefficient of restitution (e). The coefficient of restitution (e) is defined as,

$$e = -\frac{\dot{x}_n^+ - \dot{y}_n^+}{\dot{x}_n^- - \dot{y}_n^-} \tag{3}$$

Here $(\dot{x}_n^+, \dot{x}_n^-)$ are the velocities of primary structure before and after n^{th}impact. The superscript $(+)$ denotes the velocity after impact and $(-)$ denotes the velocity before impact. Similarly, $(\dot{y}_n^+, \dot{y}_n^-)$ denotes the velocities of particle before and after (n^{th}) impact. The equation of conservation of momentum for two colliding bodies can be defined as,

$$M\dot{x}_n^- + m\dot{y}_n^- = M\dot{x}_n^+ + m\dot{y}_n^+ \tag{4}$$

Combining and rearranging Eqs. 3 and 4 for the velocities of particle and primary structure after each impact gives,

$$\dot{x}_n^+ = \frac{(1-\mu e)\dot{x}_n^- + (1+e)\mu\dot{y}_n^-}{1+\mu} \tag{5}$$

$$\dot{y}_n^+ = \frac{(1+e)\dot{x}_n^- + (\mu-e)\dot{y}_n^-}{1+\mu} \tag{6}$$

Here $\mu = \frac{m}{M}$ is the mass ratio. During the numerical simulations, the impact between the primary structure and particle is determined by the following condition,

$$|x(t) - y(t)| \geq d \tag{7}$$

Where $x(t), y(t)$ are the displacements of primary structure and particle respectively. Whenever an impact is detected, the velocities of the objects change depending on the mass ratio (μ) and coefficient of restitution (e).

3. Experiments

3.1. Soft Materials

Particle impact dampers work on the principle of momentum

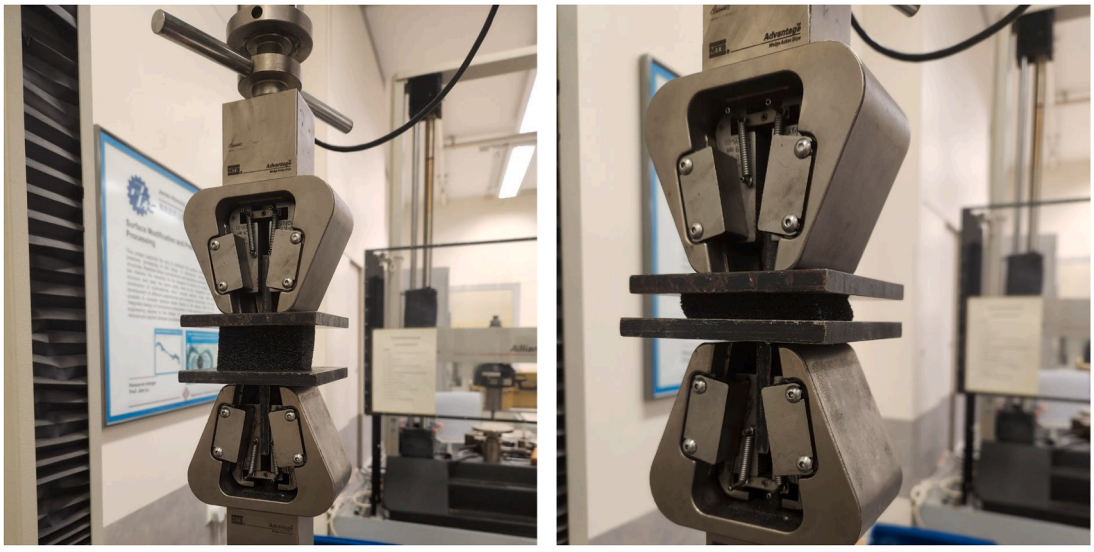

Fig. 3. Compression test picture.

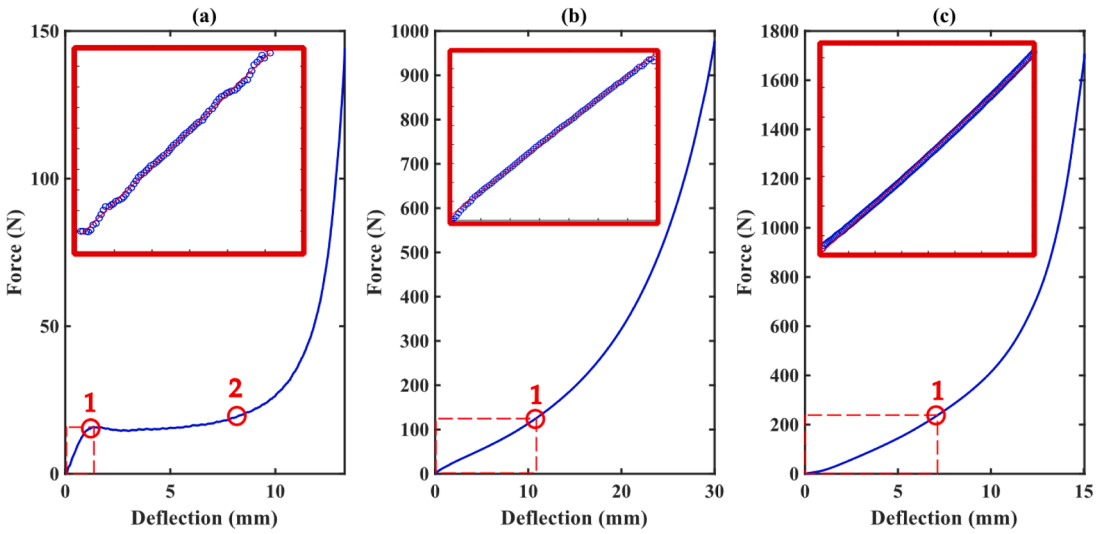

Fig. 4. Force-deflection curves of the materials (Experiment) **(a)** Polyurethane (PU) foam **(b)** Polyethene (PE) foam **(c)** Rubber.

exchange and energy dissipation through impacts. Therefore, it is necessary to adopt special materials to enhance energy dissipation at the point of impact. Three commonly used materials used in various vibration suppression applications are tested in this study [68].

The first test material is known as polyurethane (PU) foam, which is commercially known as cushioning foam [69–71], as shown in Fig. 2**a**. It is a softer, open-cell type of foam. Air can flow throughout the foam because the cells are open and not cross-linked. Such characteristics make this foam softer and enable it to absorb shock energy better. It distributes the energy more broadly.

The second test material is known as polyethylene (PE) foam, as shown in Fig. 2**b**. Polyethene foam is a closed-cell foam where the molecules are cross-linked to provide more rigidity. The crosslink character of this foam causes it to return to its original shape quickly. Which introduces a little bit of bounce in addition to the shock absorption [72,73]. Therefore, it can be considered a shock-repelling foam. The third test material is known as rubber shown in Fig. 2**c**. Most of the vibration mounts are produced with rubber because it has one of the highest levels of resilience which leads to vibration reduction.

The response of these cushioning materials to a compressive force is tested by compression tests. A common compression test uses a measurable force on the surface of the material, and the deflection is recorded as well. The compression test setup is shown in Fig. 3.

The data obtained from the compression tests are analyzed to obtain the force-deflection curve of each material, as shown in Fig. 4. It can be observed that the response of the polyurethane (PU) foam is different from the polyethene (PE) foam and rubber. Such a response can be observed in the soft materials exhibiting an energy absorption region [70,73].

Fig. 4**a** presents the response of the polyurethane (PU) foam, which is known as cushioning foam. The response up to point 1 is classified as the linear elastic region, as the deformation of the material under load is linear. Moreover, the region from point 1 to point 2 is known as the energy absorption region [74]. Lastly, the region after point 2 is classified as the densification region.

The coefficient of restitution (e) is highly important for the design of particle impact dampers. It depends on the material used at the point of impact. Experimentally, the coefficient of restitution (e) is determined by dropping the metallic ball from a known height at a surface with different materials. The rebound height of a ball after the first impact is determined by recording the whole experiment with a high-speed camera. It is understood that the rebound height can be changed by altering the thickness of these energy-absorbing materials. Therefore, each material has a similar thickness (20 mm) in these tests for consistency. Mechanical properties of the soft materials can vary with the size, shape, density, temperature, etc. Therefore, considering all these parameters for energy dissipation can become highly complicated. The coefficient of restitution (COR) can depend on several factors, such as impact velocity and material properties, and may be nonlinear. In this study, COR is assumed constant for simplicity, and the close agreement between experimental and numerical results supports this assumption within the tested range. The coefficient of restitution can be determined by the equation given below after knowing the initial and final height of the ball after bouncing,

Table 1
Coefficient of restitution (e) of different impact surfaces.

Impact Material	Coefficient of restitution (e)
Aluminium	0.82
Acrylic	0.72
Steel	0.80
Rubber	0.70
Polyethylene (PE) foam	0.68
Polyurethane (PU) foam	0.36

$$e = \sqrt{\frac{H_f}{H_i}} \tag{8}$$

Where H_f and H_i are the final and initial heights of the ball. The rebound tests are repeated three times, and the average is calculated to avoid any human error. The calculated coefficients of restitution with different impact surfaces are presented in Table 1.

It can be observed from Table 1 that the largest magnitude of the coefficient of restitution is measured when there is a metallic surface (Aluminium). On the other hand, the minimum magnitude of the coefficient of restitution is measured when a soft cushioning material (Polyurethane foam) is used as the impact surface. Interestingly, rubber and polyethylene (PE) foam show a similar COR to the hard impact materials. When the ball strikes the surface of rubber and PE foam, a spring-like response can be observed during the experiments. Therefore, a large rebound height is recorded compared to the polyurethane (PU) foam. It should be noted that factors such as material durability, creep resistance, temperature stability and long-term aging are not considered in this study, as the focus is on the effect impact surfaces on damping performance. Furthermore, formal noise measurements were not conducted, the damping system was observed to operate without noticeable audible noise during the experiments.

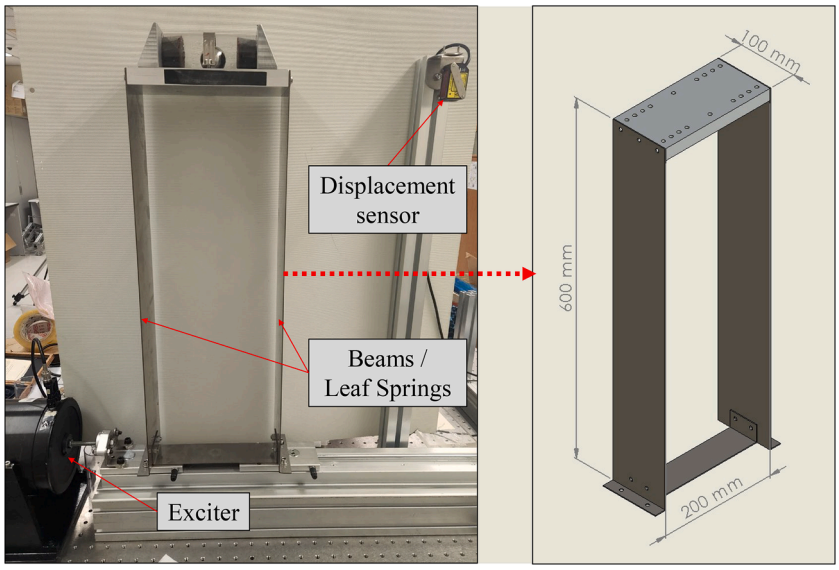

Fig. 5. Experimental setup of a single degree of freedom system equipped with a particle impact damper.

Table 2
Parameters of the primary structure.

Parameter	Magnitude
Mass (M)	2.82 Kg
Natural frequency (f)	2.84 Hz
Damping ratio (ζ)	0.003

3.2. Methodology

A single degree of freedom (SDOF) structure is manufactured to test the particle impact damper with different surfaces (Hard and Soft) at the point of impact. The structure includes two beams acting as leaf springs, and a mass at the top. Moreover, an exciter is installed to generate the vibrations, as shown in Fig. 5.

A particle impact damper (PID) is developed by installing two stoppers at the top of the primary structure. A transparent acrylic tube with a metallic ball inside is used as the PID in these experiments. The materials can be installed at either end of the stopper to provide different impact surfaces during the vibrations.

The system parameters are identified through the free vibration experiment. The structure is provided with an initial displacement and the free vibration response without any external damping is recorded.

The results obtained from the free vibration analysis are presented in Fig. 7, where Fig. 7(a) shows the displacement of the structure and Fig. 7 (b) shows the FFT spectra obtained from the displacement response. The FFT analysis of the displacement data provides the natural frequency (f) of the primary structure. Moreover, the response of the structure shows that there is some internal damping present in the displacement of the structure. Therefore, the damping ratio (ζ) is determined with the logarithmic decrement method. Furthermore, the system parameters are shown in Table 2.

The experiments are conducted on the structure and particle impact damper with different contact surfaces. All experiments were conducted at a single resonance frequency, which limits the generalizability of the conclusions. This focused approach enables a detailed time-domain analysis and provides deeper insight into the mechanisms of particle impact damping and the effect of different materials. A sinusoidal force at the resonance frequency ($2.84\ Hz$) of the primary structure is provided with the exciter and the amplitude is kept is constant at 2 mm for all experiments for the consistency. The displacement of the structure is recorded through a contactless displacement sensor. A force sensor is installed on each stopper to record the force felt by the structure at each impact, as shown in Fig. 6. The impact force varies with the use of different cushioning materials. The length of the cavity ($d = 60\ mm$), excitation force magnitude, and mass ratio (μ) are kept constant for all experiments to study the effect of cushioning materials solely. The thickness of the surface is 15 mm for all materials.

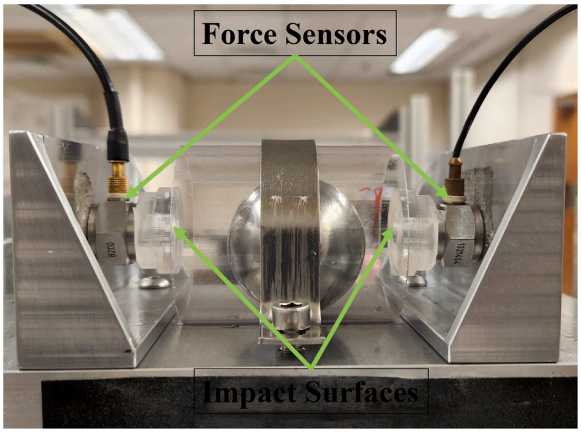

Fig. 6. Prototype of the particle impact damper attached to the SDOF structure.

4. Results and discussions

The results obtained from the experiments and numerical model are presented in this section. The numerical model with the coefficient of restitution (e) to model the cushioning material is used to simulate the response of the primary structure. Moreover, the parameters of each experiment are used in the simulations to compare the results. The damping performance of the particle impact damper with different impact surfaces is presented and discussed below.

4.1. Hard Impact

1. Aluminium

First, Aluminium is used as the impact surface material between the particle and primary structure. The coefficient of restitution between the

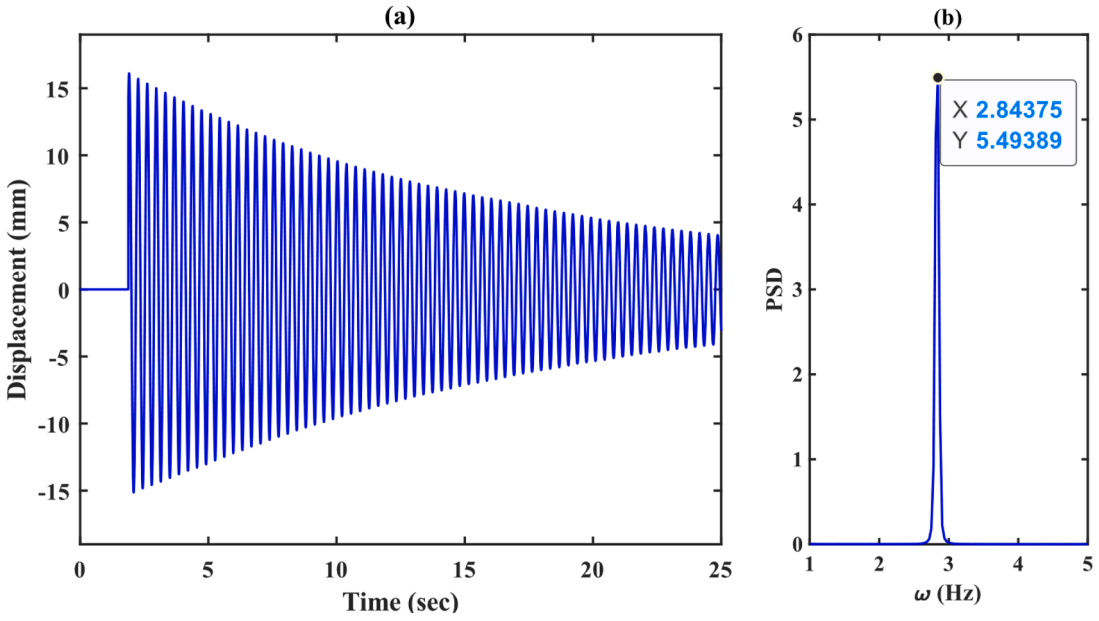

Fig. 7. **(a)** Experimental free vibration response of the structure without damping **(b)** FFT spectra.

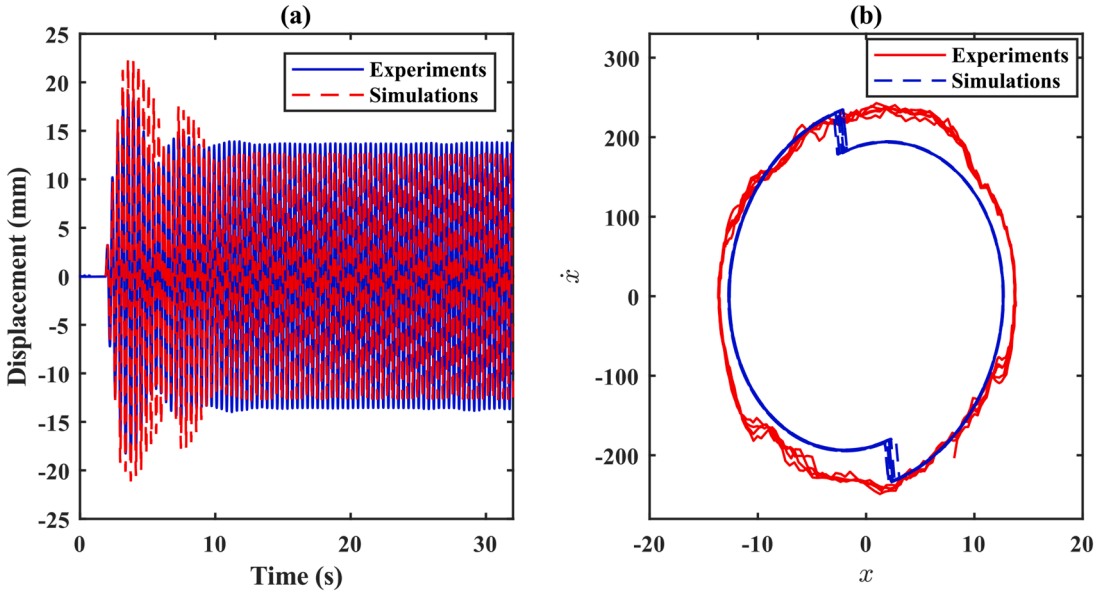

Fig. 8. **(a)** Displacement of the primary structure with Aluminium as the impact surface ($e = 0.82$) **(b)** Stability (displacement-velocity) plot of the primary structure in the steady-state region.

steel ball and the Aluminium surface is determined by experiments, as shown in Table 1. This magnitude is used in the numerical model to simulate the response of the primary structure.

The displacement of the primary structure recorded from the experiments and numerical simulations is presented in Fig. 8 (a). The results show that the results from numerical simulations matches well with the experimental results considering the nonlinearities involved in the system. Furthermore, the system seems to stabilize after passing the transient phase of vibrations and a steady-state response is evident after it. The initial transient phase is a natural characteristic of dynamic systems before steady-state motion is established. In the present case, this behavior is further influenced by the clearance in the particle damper, which delays the first impact. After the displacement exceeds the clearance and particle collisions commence, the system gradually stabilizes into steady-state vibration with sustained energy dissipation.

The stability plot (displacement-velocity) of the primary structure with a displacement-velocity diagram is presented in Fig. 8 (b). The plot shows that the impact with the particle and change in velocity occurs at the same position in the steady-state region. The displacement of the primary structure and the impact with the particle synchronize after the first peak of the displacement, eliminating any chances of disorganized motion between two masses. The stability plot of the primary structure obtained from the experiments and numerical model is compared in Fig. 8 (b) as well.

One of the identified problems with the particle impact damper is associated with high-intensity impact. Each impact induces stresses to the primary structure, and it could be harmful to some vulnerable/weak structures. Therefore, the force experienced by the primary structure at each impact is measured by the force sensors installed on the other side of the stoppers. When there is no cushioning material installed on the

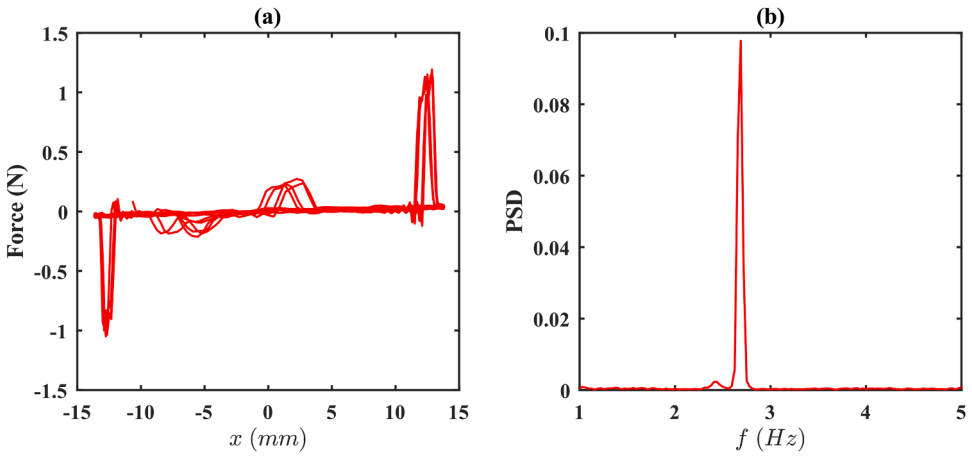

Fig. 9. **(a)** Displacement-Force plot of the primary structure (Experiments) **(b)** PSD of the force data.

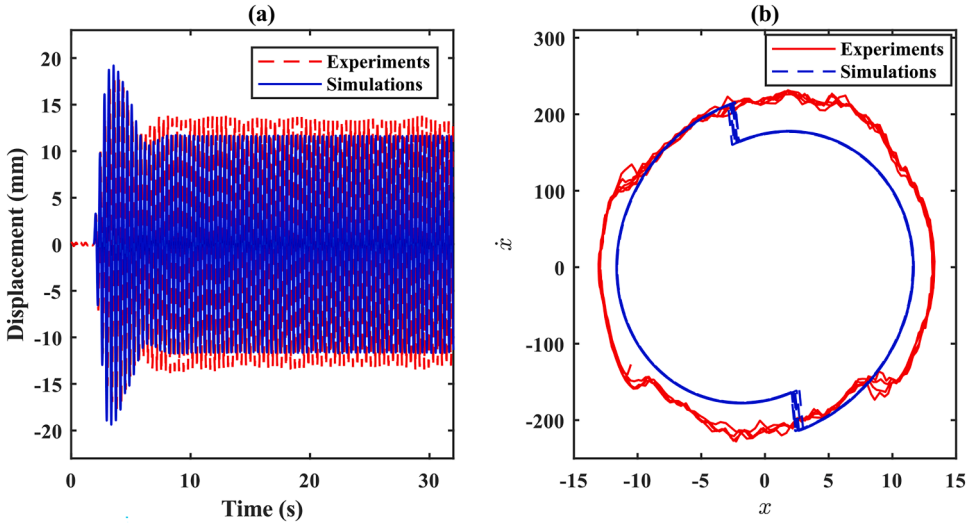

Fig. 10. **(a)** Displacement of the primary structure with Steel as the impact surface ($e = 0.80$) **(b)** Stability (displacement-velocity) plot of the primary structure in the steady-state region.

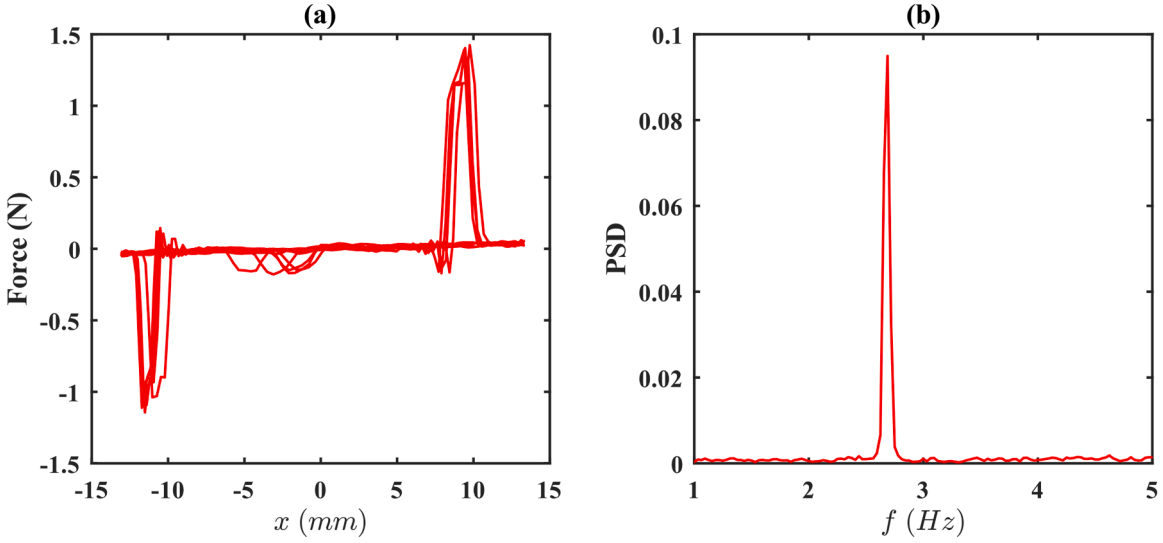

Fig. 11. **(a)** Displacement-Force plot of the primary structure (Experiment) **(b)** PSD of the force data.

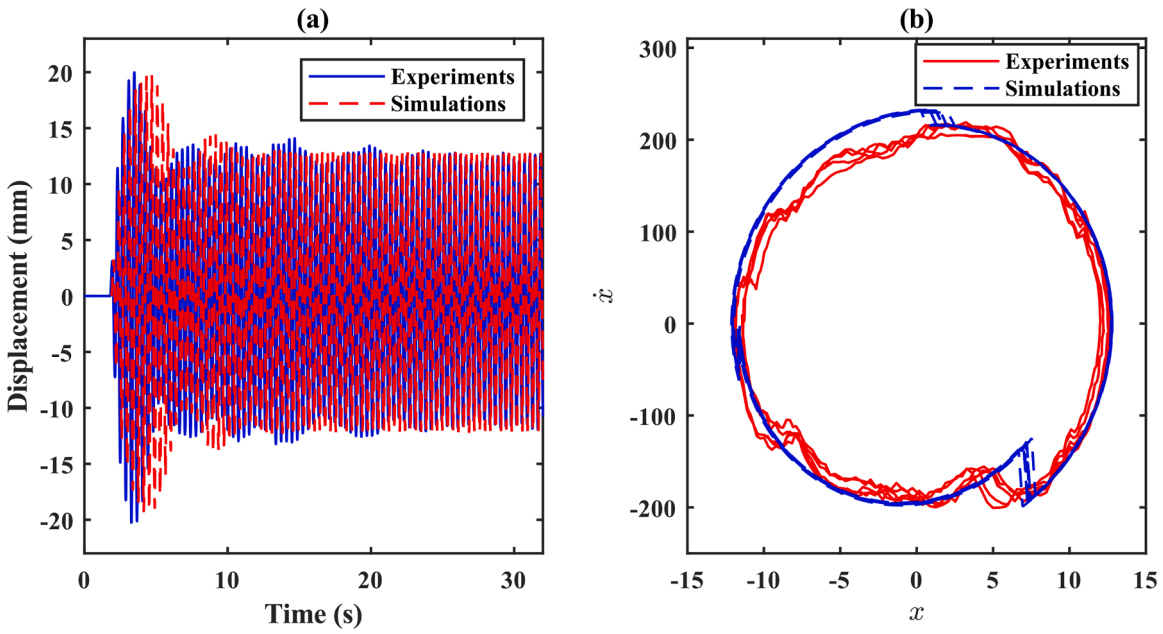

Fig. 12. **(a)** Displacement of the primary structure with Acrylic as the impact surface ($e = 0.72$) **(b)** Stability (displacement-velocity) plot of the primary structure in the steady-state region.

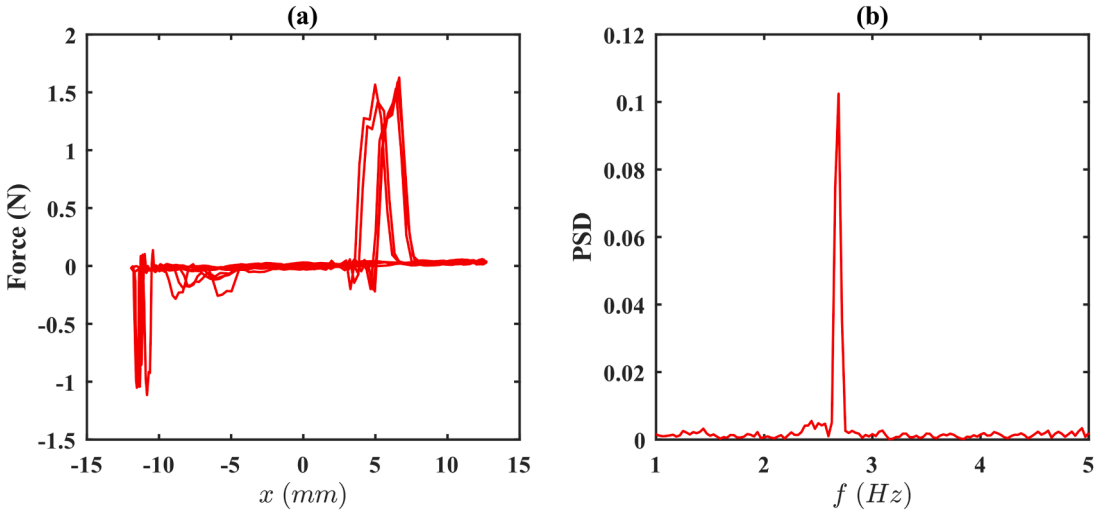

Fig. 13. **(a)** Displacement-Force plot of the primary structure (Experiment) **(b)** PSD of the force data.

impact surface, the impact force can be higher and more dangerous for the structure as it is a repetitive force. Furthermore, the negative force values in the Fig. 9 indicate the direction of impact within the particle damper cavity; forces on opposite sides of the cavity are assigned opposite signs for clarity. The displacement-force plot is presented in Fig. 9 (a), while the spectral density of the force data is presented in Fig. 9 (b). The spectra show that most impacts occur at a frequency close to the natural frequency of the primary structure.

2. Steel

In the next experiment, steel is used between the particle and the primary structure. Steel has a similar magnitude of the coefficient of restitution ($e = 0.80$) as aluminium. The displacement of the primary structure recorded from the experiments and numerical model is presented in Fig. 10. It can be observed that the steady-state amplitude is closer to the previous case.

Furthermore, the force experienced by the primary structure through impacts is recorded and presented in Fig. 11 (a). It can be observed that the magnitude of the force is identical to the previous case. Additionally, the FFT of the time-series force data shown in Fig. 11 (b) shows that the impact frequency strictly follows the vibration frequency.

3. Acrylic

The third test material for the hard impact is used as acrylic. Acrylic is a commonly used material in various mechanical applications due to its various advantages. The coefficient of restitution of the acrylic is measured as $e = 0.72$. The coefficient of restitution is slightly lower than the other two metallic surfaces. Acrylic is rigid, and a hard impact is generated at each collision. The displacement of the primary structure with acrylic in the PID is presented in Fig. 12 (a). While the stability plot of the structure is presented in Fig. 12 (b).

The force experienced by the primary structure using acrylic as the

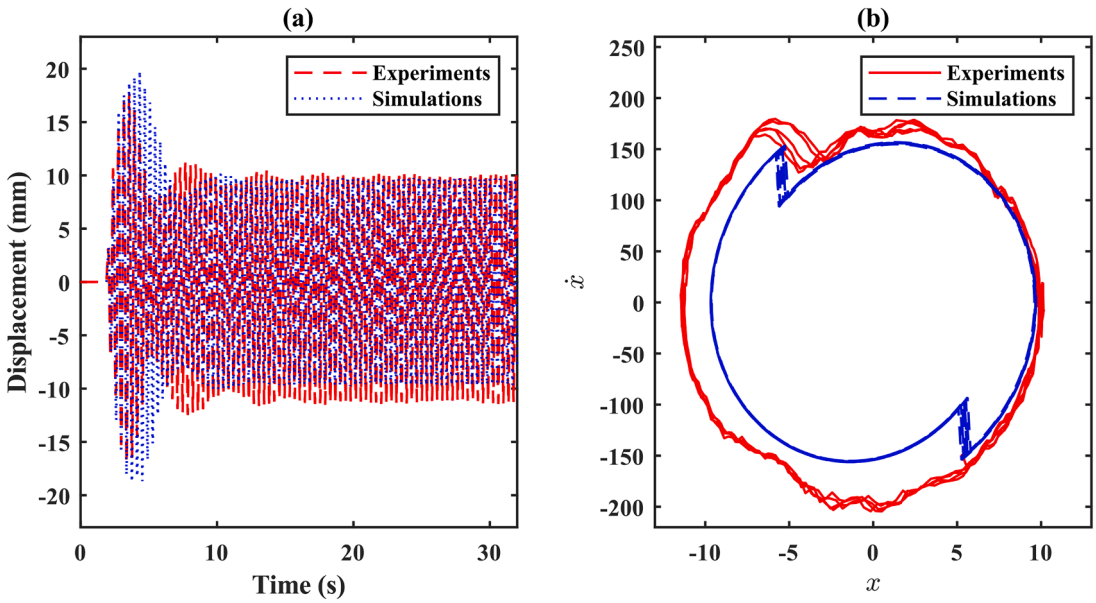

Fig. 14. **(a)** Displacement of the primary structure with rubber ($e = 0.70$) as the impact surface in PID **(b)** Stability (displacement-velocity) plot of the primary structure in the steady-state region.

impact surface is presented in Fig. 13 (a). The magnitude of the force is slightly lower than the other two hard-impact surfaces. It can be observed that the contact force magnitude is highly related to the coefficient of restitution of the material.

4.2. Soft impact

4. Rubber

A stopper with rubber installed on the collision side is installed to provide a softer surface for the impact. Rubber is a widely used material in vibration isolation applications. The material properties of the rubber can change abruptly with the environmental conditions, which makes it challenging to model the response of such materials. Therefore, it is assumed in the numerical model that the coefficient of restitution and temperature is constant throughout the operation of the particle impact damper.

From the force-deflection plot of rubber in Section 3.1, it can be observed that the rubber shows the densification region quickly. The deformation remains linear against the limited force but quickly becomes nonlinear with a parabolic response. The inner structure of the rubber densifies after a limited force, and it requires excessive force to deform the rubber after that. One of the advantages of rubber can be observed is that it has a long elastic region and can recover the initial shape even after a huge force. The response of the rubber is tested in the coefficient of restitution experiments, and the magnitude is measured as 0.70. Compared with the hard impact (Aluminium), the rubber shows relatively higher energy dissipation in impact.

The displacement of the primary structure while using rubber as the cushioning material is plotted in Fig. 14 (a). The plot shows that the results from experiments match the numerical results with ($e = 0.70$). The coefficient of restitution of the rubber is still higher due to its elastic properties. A spring-like response has been observed which adds to the energy of the particle motion at each impact. This shows that the coefficient of restitution is highly influential on the outcome of particle impact damper, and precise care is required during the designing process. On the other hand, the stability (displacement-velocity) plot is shown in Fig. 14 (b) with experimental and simulation data. Compared

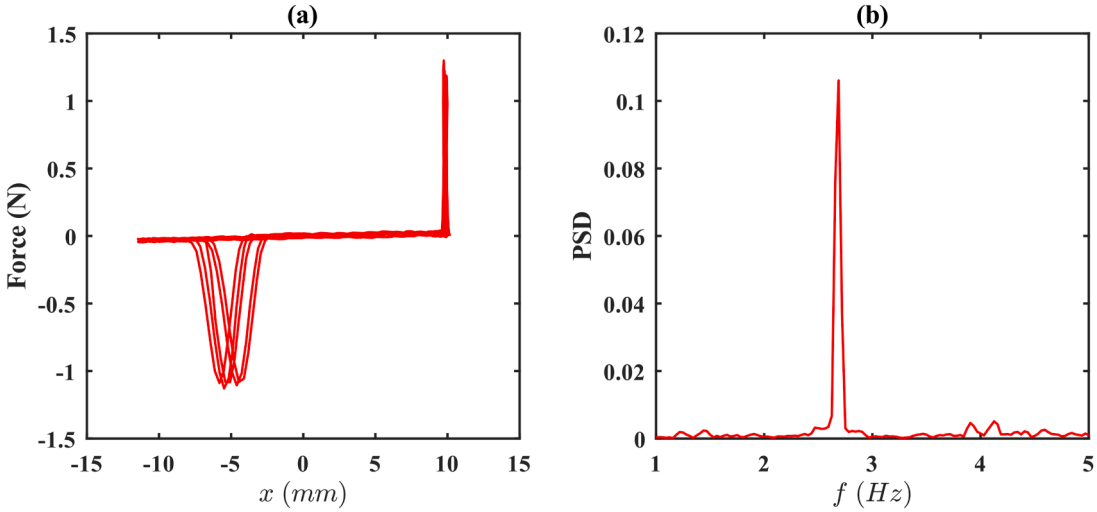

Fig. 15. **(a)** Displacement-Force plot of the primary structure with rubber as cushioning material (Experiment) **(b)** PSD of the force data.

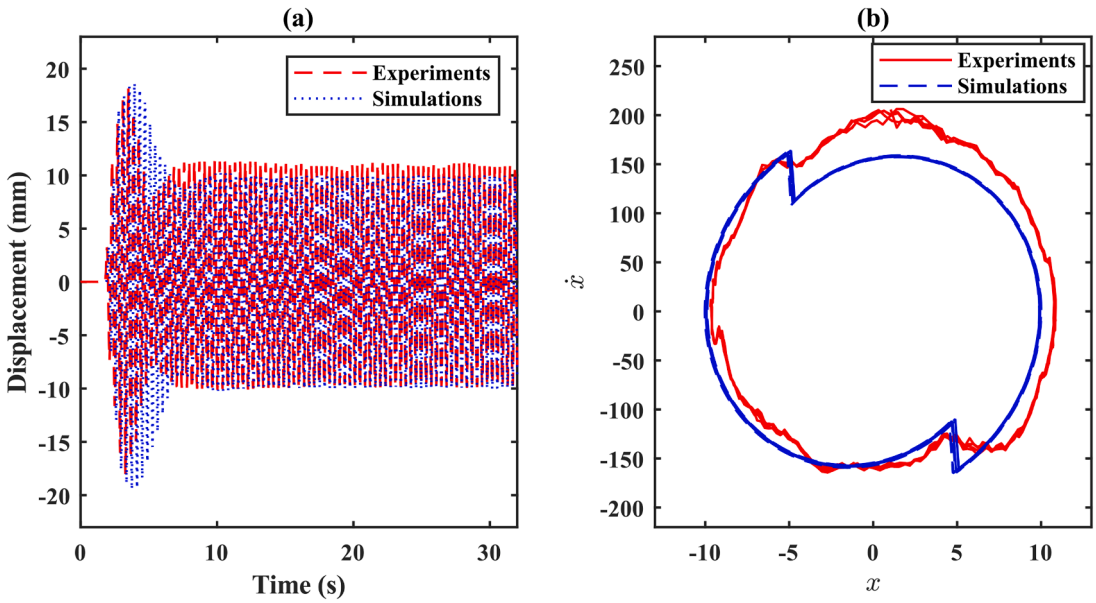

Fig. 16. **(a)** Displacement of the primary structure with PE foam ($e = 0.68$) as the impact surface in PID **(b)** Stability (displacement-velocity) plot of the primary structure in the steady-state region.

with the hard impact, the impact occurs in multiple locations due to the beating phenomenon during the steady-state region.

The force experienced by the primary structure is recorded with the force sensors attached to the stoppers. The displacement-force plot is presented in Fig. 15 (a). Compared with the hard impact (Section 4.1), the magnitude of the force exerted on the primary structure is reduced significantly. A smaller force exerted on the primary structure during operation can assure the protection of the structure by using a particle impact damper. One of the concerns of using rubber can be associated with vibration reduction performance, as the amplitude of the displacement is not reduced significantly. Furthermore, the FFT analysis of the force data provides the frequency of impact, as shown in Fig. 15 (b). It can be observed that the impacting frequency is close to the natural frequency of the structure.

5. Polyethylene (PE) foam

Polyethylene (PE) foam is commonly used in packaging. It is considered the shock-repellent kind of foam of its properties. Looking at the force-deflection curve of PE foam (Section 3.1), a similar response as the rubber can be observed. Moreover, the coefficient of restitution is measured near that of rubber. Therefore, a similar response to the rubber can be expected by using PE foam as the cushioning material in the particle impact damper.

Displacement of the primary structure while using PE foam as the cushioning material in PID is presented in Fig. 16 (a). The results from numerical simulations and experiments show a similar response to the rubber as the cushioning material. The influence of the design parameters especially the coefficient of restitution and clearance can be considered highly complicated. It is challenging to describe the relationship between these parameters and the performance of PID. Fixing the clearance and altering the coefficient of restitution only show that the response can change drastically with a slight change in the coefficient of restitution (e). On the other hand, the stability plot of the primary structure in the steady-state region can be seen in Fig. 16 (b). The plot shows that there are impacts at more than two locations due to the

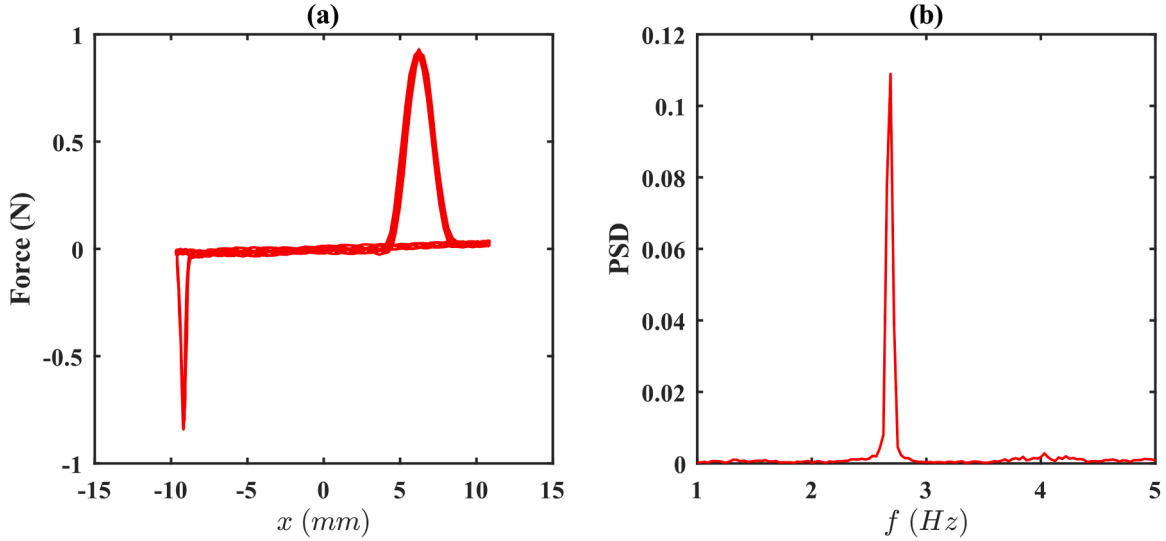

Fig. 17. **(a)** Displacement-Force plot of the primary structure with PE foam as cushioning material (Experiment) **(b)** PSD of the force data.

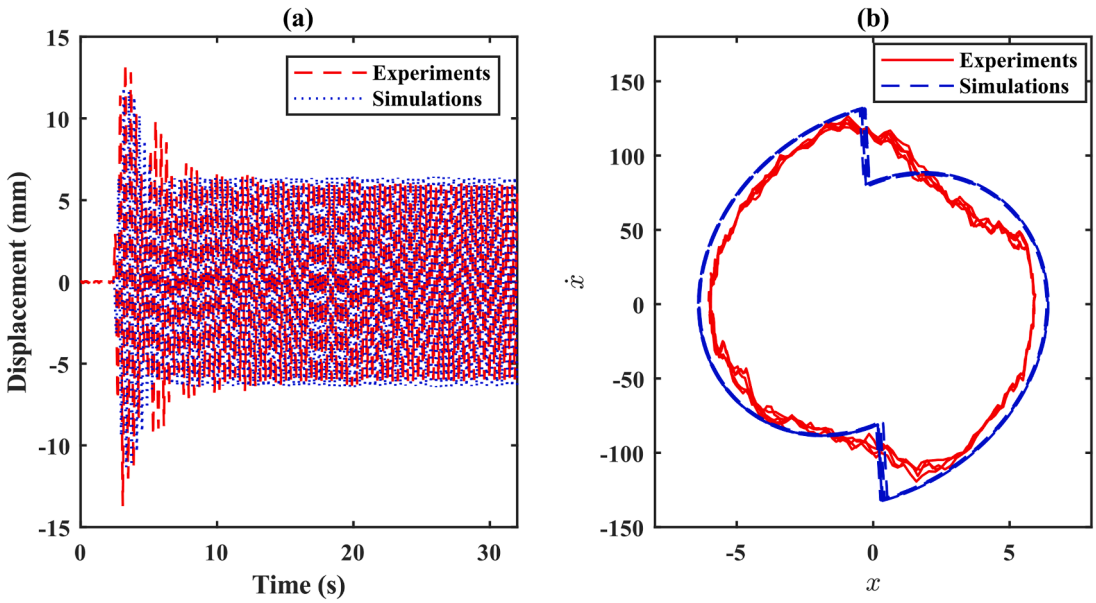

Fig. 18. **(a)** Displacement of the primary structure with PU foam ($e = 0.36$) as the impact surface in PID **(b)** Stability (displacement-velocity) plot of the primary structure in the steady-state region.

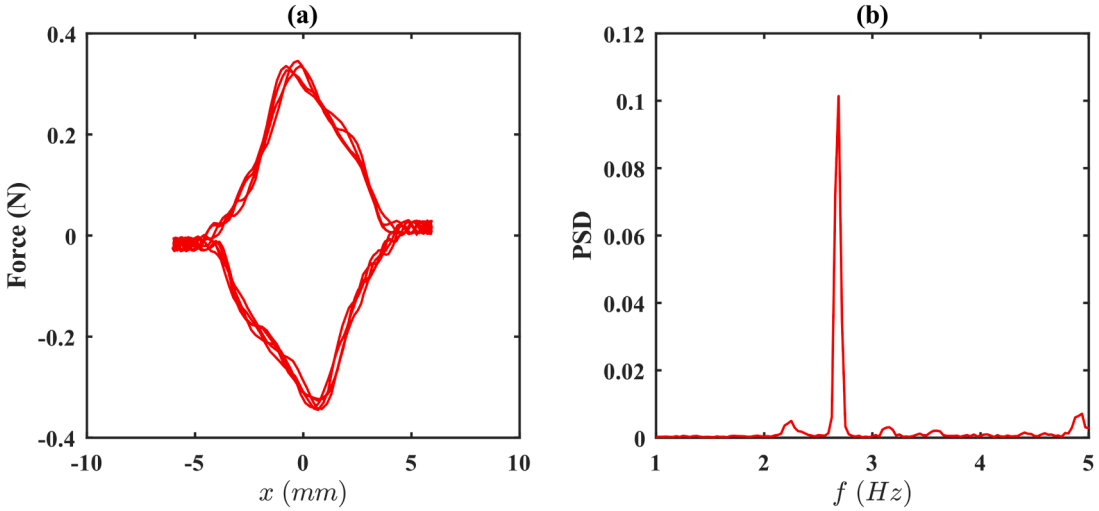

Fig. 19. **(a)** Displacement-Force plot of the primary structure with PU foam as cushioning material (Experiment) **(b)** PSD of the force data.

presence of beating phenomena. It is understood that the beating phenomenon occurs due to misaligned design parameters. The steady-state response requires an aligned combination of design parameters, where the motion of the particle synchronizes with the motion of the primary mass.

The displacement-force plot is presented in Fig. 17 (a), while the FFT analysis of the force data is shown in Fig. 17 (b). The magnitude of the force experienced by the primary structure through impacts with PE foam is identical to the rubber. The magnitude decreases significantly compared to the hard impact. The displacement amplitude with PE foam and rubber can be acceptable in some applications but there is still room for improvement.

6. Polyurethane (PU) foam

Polyurethane (PU) foam can be considered the actual cushioning foam in industrial applications. It is softer than PE foam and rubber with soft nature. The force-deflection curve of PU foam (Section 3.1) shows a slightly different response compared to PE foam and rubber. The Energy-absorbing region was only seen during the compression test of PE foam compared to the other cushioning materials. Therefore, this foam can be considered the softer of them all. Furthermore, the energy absorption is verified from the coefficient of restitution tests. The coefficient of restitution of the PU foam is $e = 0.36$, which is the lowest among these materials.

The displacement of the primary structure with PU foam in PID is presented in Fig. 18 (a). The graph shows that the amplitude of the displacement reduces significantly with PU foam as the energy dissipation increases. Furthermore, the stability (displacement-velocity) diagram presented in Fig. 18 (b) shows that there are two impacts only in each cycle during the steady-state region. It can be concluded from the graphs that the softer material dissipates more energy through the impacts in PID, which leads to the less disorganized motion of particles. Hence, the particle will have a significantly synchronized motion with the primary mass leading to a more stable response.

The displacement-force plot from the experiments is presented in Fig. 19 (a), which shows that the magnitude of the force experienced by the structure is reduced further by using polyurethane (PU) foam in the

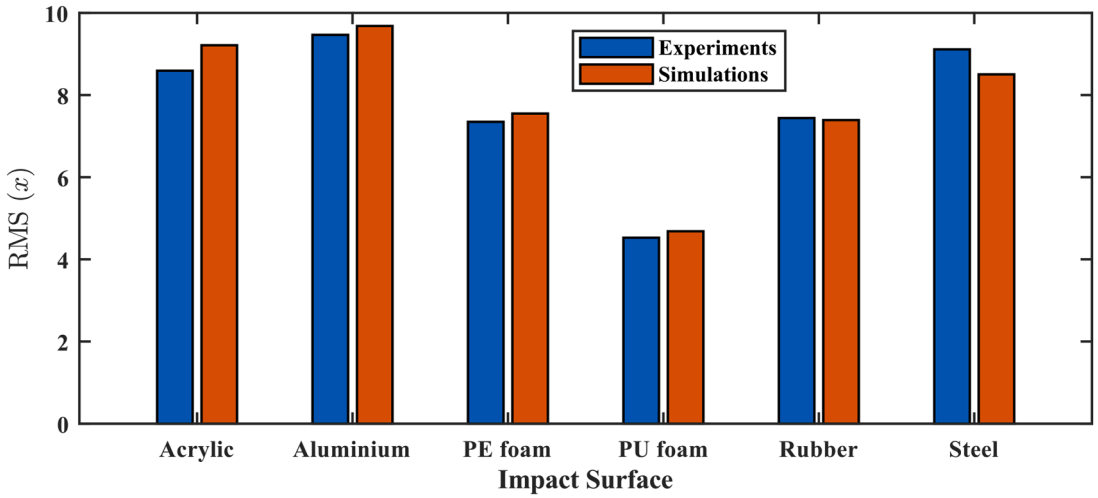

Fig. 20. Comparison of the RMS displacement of the primary structure with different impact surfaces in particle impact damper.

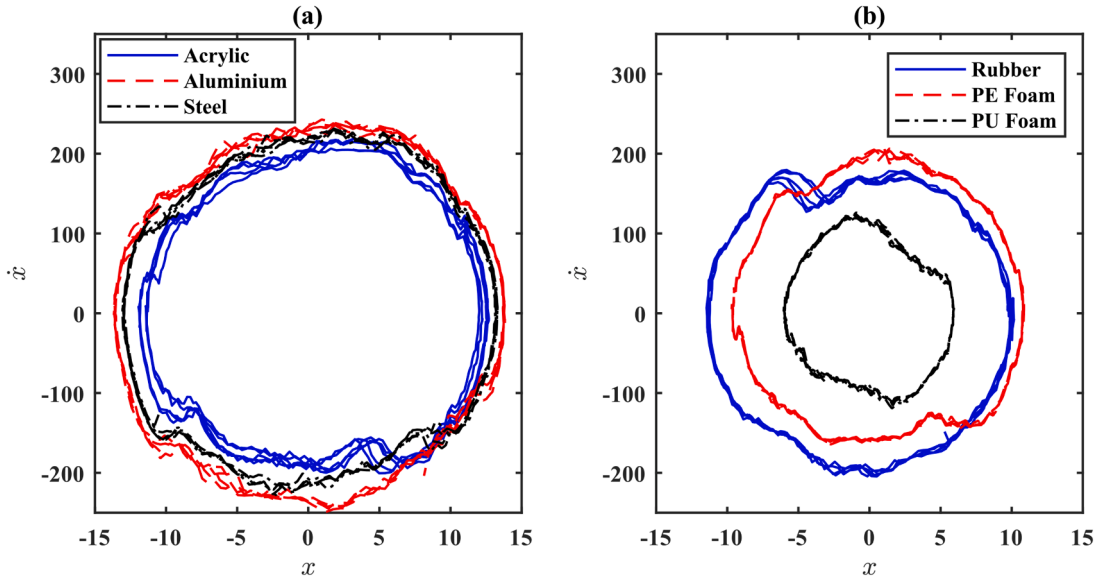

Fig. 21. (a) Displacement-Velocity plots of the primary structure with Hard Impacts (Experiment) **(b)** Displacement-Velocity plots of the particle impact damper with soft impacts (Experiment).

PID. The softer nature of the foam absorbs most of the impact energy and protects the primary structure. Moreover, PU foam can protect vulnerable structures without compromising the performance of PID. Additionally, Fig. 19 (b) shows the spectral density of the force data, which shows that the impacting frequency is matching with the natural frequency of the primary structure. It is understood that irrespective of the impacting material, the frequency of impact follows the frequency of vibrations.

4.3. Discussion

The performance of the particle impact damper attached to the single degree of freedom is studied with different impact surfaces in Section 4.1 and 4.2. The displacements of the primary structure with different impacting surfaces in PID from experiments are compared in Fig. 20. In this figure, the rms displacement magnitude recorded from numerical simulations and experimental data is compared. Maximum error % among the presented results is calculated as 7.14% which lies within acceptable range considering the several nonlinear phenomena involved in the system. The results show a good agreement validating the numerical model.

The maximum RMS amplitude is achieved with Aluminium as the impact surface between the particle and primary mass. It is directly related to the coefficient of restitution of the material. It is well understood that the higher COR promotes the momentum exchange and lesser energy absorption at impacts. The principle of damping of PID consists of momentum exchange and energy absorption at impacts. Therefore, a balanced combination of energy absorption and momentum exchange is required to maximize the performance. The minimum displacement amplitude is achieved when using PU foam ($e = 0.36$) as the cushioning material in PID.

Furthermore, it is determined that the amplitude of the displacement can be reduced to 52 % by choosing a proper material for the impact surface. Additionally, it is also proved that the understanding of the material selection is necessary for maximum vibration suppression as all the cushioning materials are not guaranteed to improve the performance.

The stability of the vibration is another parameter to justify the effect of any damper associated with a structure. The results from each cushioning material verify that the system stability during the vibrations is

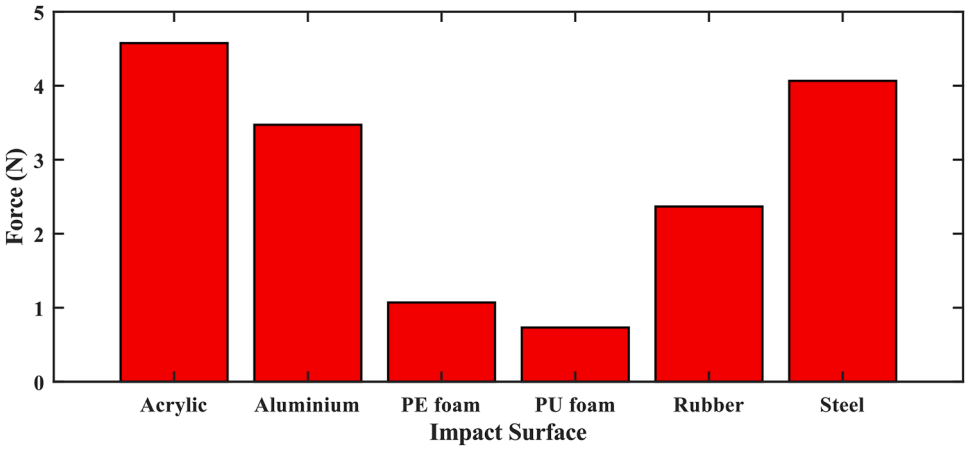

Fig. 22. Comparison of the impact force experienced by the primary structure during operation (Experiment).

Table 3
Comparison of the amplitude reduction with different surface materials in PID.

Surface material	Coefficient of restitution (e)	Amplitude reduction
Aluminium	0.82	—
Acrylic	0.72	09.20 %
Steel	0.80	03.71 %
Rubber	0.70	21.38 %
Polyethylene (PE) Foam	0.68	22.35 %
Polyurethane (PU) Foam	0.36	52.16 %

appropriate. The comparison of the displacement-velocity plots is presented in Fig. 21 (a) for the different hard impacts. The slight bumps in the velocity plot show the effect of an impact. It can be observed that the hard impacts have unorganized impacts throughout the motion of the structure. In addition, few impacts are adding to the system's energy rather than dissipation. On the other hand, Fig. 21 (b) shows the displacement-velocity plot of soft impacts. The standout is that there are a clear two impacts per cycle evident in the plot. Although more than two impacts per cycle are possible, the most effective impacts are only two in each cycle and occurring at a similar position. Additionally, there is no visible spike showing the energy added to the primary structure through impacts.

It can be observed that the minimum velocity amplitude is achieved when polyurethane (PU) foam is used as the soft impact material. The coefficient of restitution of PU foam is 0.36, which leads to balanced momentum exchange and energy dissipation through impacts. It is worth noting that any soft impact material improves the performance of the particle impact damper. Furthermore, a clear understanding of the effects of hard and soft materials on the performance of PID is required to achieve maximum vibration attenuation.

On the other hand, the force exerted on the primary structure during the operation of PID is compared in Fig. 22 for different impact surfaces. It can be concluded that the larger impact force cannot be related to better damping performance. The larger impact force is rather related to inducing high local stress to the primary structure through impacts, which might be harmful to some vulnerable structures.

The maximum RMS displacement magnitude is observed with Aluminium as the impact surface. The RMS displacement of the vibrations is compared with Aluminium to compare the performance of different materials, and the results are presented in Table 3. It can be observed that the soft impact outperforms the hard impact surfaces. Additionally, an accurately selected soft impact material (PU foam in this study) can reduce the amplitude of vibrations to 52 %.

5. Conclusion

This study demonstrates the critical influence of the impact material on the performance of particle impact dampers. Experimental and numerical investigations were carried out using three commonly applied soft materials, rubber, polyethylene (PE) foam, and polyurethane (PU) foam as impact surfaces, and compared with traditional hard impacts (Aluminium, Steel, Acrylic). The experimental results were further validated with a simplified numerical model incorporating the experimentally measured coefficients of restitution. The findings indicate that larger contact forces do not necessarily result in higher damping efficiency. Rubber and PE foam exhibited long elastic deformation regions and spring-like, shock-repellent behavior, but their damping performance was lower than that of hard impacts. In contrast, PU foam, with its energy absorption properties and lowest coefficient of restitution among the tested materials, achieved a vibration amplitude reduction of up to 42%. These results underscore the importance of carefully selecting the impact material to optimize PID performance, minimize structural damage, and reduce operational noise. By addressing the previously underexplored role of the impact surface, this study provides practical guidance and novel insights for designing PIDs for maximum vibration attenuation and structural protection.

Data availability

The data used in the manuscript can be shared on a reasonable request from the corresponding author.

CRediT authorship contribution statement

Muhammad Ayaz Akbar: Writing – original draft, Validation, Software, Methodology, Investigation, Formal analysis, Data curation, Conceptualization. **Hassan Raza:** Writing – review & editing, Writing – original draft, Visualization, Supervision, Resources, Project administration, Investigation, Formal analysis, Data curation, Conceptualization. **Naveed Husnain:** Writing – review & editing, Supervision, Resources, Project administration, Methodology, Formal analysis, Conceptualization.

Declaration of competing interest

The authors declare that they have no conflict of interest.

Acknowledgement

Author would like to acknowledge the support from The Hong Kong Polytechnic University, Hong Kong SAR and University of Trento, Italy

for the laboratory access. Authors would also like to acknowledge the support from Shenzhen MSU-BIT University, Shenzhen during this research.

Data availability

Data will be made available on request.

References

[1] K.T. Tran, et al., Vibration isolation using inerter-induced negative effective mass: an experimental and theoretical study, Results. Eng. (2025) 107188.
[2] J. Sadeghi, Z. Valipouri, M. Esmaeili, Effect of building stiffness and mass distribution on underground railway-induced vibration, Results. Eng. 26 (2025) 104910.
[3] S. Yaghoubi, A. Ghanbarzadeh, Modeling and optimization of car suspension system in the presence of magnetorheological damper using Simulink-PSO hybrid technique, Results. Eng. 22 (2024) 102065.
[4] A.B.M. Omar, et al., Torsional vibration control in diesel engine-driven centrifugal pump: validation through experimental results, Results. Eng. 24 (2024) 103549.
[5] M. Basili, F. Busato, M. De Angelis, Integrated seismic and energetic rehabilitation of existing buildings based on the tuned mass damper concept, Results. Eng. 24 (2024) 103552.
[6] L. Gagnon, M. Morandini, G.L. Ghiringhelli, A review of particle damping modeling and testing, J. Sound. Vib. 459 (2019).
[7] R.D. Friend, V.K. Kinra, Particle impact damping, J. Sound. Vib. 233 (1) (2000) 93–118.
[8] C.N. Bapat, S. Sankar, Single unit impact damper in free and forced vibration, J. Sound. Vib. 99 (1) (1985) 85–94.
[9] Z. Lu, et al., Particle impact dampers: past, present, and future, Struct. Control Health Monit. 25 (1) (2018).
[10] Z. Lu, K. Li, Y. Zhou, Comparative studies on structures with a tuned mass damper and a particle damper, J. Aerosp. Eng. 31 (6) (2018).
[11] M. Saeki, Impact damping with granular materials in a horizontally vibrating system, J. Sound. Vib. 251 (1) (2002) 153–161.
[12] R. Ibrahim, Vibro-impact Dynamics: Modeling, Mapping and Applications, 43, Springer-Verlag, Berlin Heidelbergs, 2009.
[13] O.K. Soureshjani, S.H. Hosseini Lavassani, Performance of tuned particle impact damper and tuned mass damper seismic control systems considering mainshock-aftershock, Structures 56 (2023) 104924.
[14] B. Wang, et al., Test and analysis of multi-cavity particle damper for vertical vibration control of pipeline structures, Eng. Struct. 281 (2023) 115744.
[15] Z. Lu, et al., Discrete element method simulation and experimental validation of particle damper system, Eng. Comput. 31 (4) (2014) 810–823.
[16] G. Michon, A. Almajid, G. Aridon, Soft hollow particle damping identification in honeycomb structures, J. Sound. Vib. 332 (3) (2013) 536–544.
[17] K. Chehaibi, C. Mrad, R. Nasri, Collision modeling of single unit impact absorber for mechanical systems vibration attenuation, J. Theor. Appl. Mech. 57 (4) (2019) 947–956.
[18] C. Snoun, M. Trigui, Design parameters optimization of a particles impact damper, Int. J. Interact Des. Manuf. Ijidem. 12 (4) (2018) 1283–1297.
[19] N. Meyer, R. Seifried, Systematic design of particle dampers for transient vertical vibrations, Granul. Matter. 25 (1) (2023).
[20] F. Terzioglu, J.A. Rongong, C.E. Lord, Influence of particle sphericity on granular dampers operating in the bouncing bed motional phase, J. Sound. Vib. 554 (2023) 117690.
[21] T. Kuriyama, M. Saeki, Investigation of dynamic characteristics of rolling particle dampers, J. Vib. Control 27 (19-20) (2021) 2243–2252.
[22] Y. Badri, et al., Experimental and numerical investigation of damping in a hybrid automotive damper combining viscous and multiple-impact mechanisms, J. Vib. Control 28 (23-24) (2021) 3676–3687.
[23] A. Papalou, S.F. Masri, An experimental investigation of particle dampers under harmonic excitation, J. Vib. Control 4 (4) (2016) 361–379.
[24] T.A. Jadhav, P.J. Awasare, Enhancement of particle damping effectiveness using multiple cell enclosure, J. Vib. Control 22 (6) (2014) 1516–1525.
[25] E.O. Steven, An analytical particle damping model, J. Sound. Vib. (2003).
[26] M.A. Akbar, H. Raza, Advanced damping solutions for single-particle impact dampers: exploring design parameters with a linear contact approach, Eng. Res. Express 7 (3) (2025) 035503.
[27] C.X. Wong, M.C. Daniel, J.A. Rongong, Energy dissipation prediction of particle dampers, J. Sound. Vib. 319 (1-2) (2009) 91–118.
[28] Z. Xu, M.Y. Wang, T. Chen, Particle damping for passive vibration suppression: numerical modelling and experimental investigation, J. Sound. Vib. 279 (3-5) (2005) 1097–1120.
[29] M. Saeki, Analytical study of multi-particle damping, J. Sound. Vib. 281 (3-5) (2005) 1133–1144.
[30] M.R. Duncan, C.R. Wassgren, C.M. Krousgrill, The damping performance of a single particle impact damper, J. Sound. Vib. 286 (1-2) (2005) 123–144.
[31] Z.W. Xu, M.Y. Wang, T.N. Chen, A particle damper for vibration and noise reduction, J. Sound. Vib. 270 (4-5) (2004) 1033–1040.
[32] X.H. Huang, et al., Equivalent model and parameter analysis of non-packed particle damper, J. Sound. Vib. 491 (2021).
[33] Z. Lu, X. Lu, S.F. Masri, Studies of the performance of particle dampers under dynamic loads, J. Sound. Vib. 329 (26) (2010) 5415–5433.
[34] S.M. Kun, K.K. Vikram, Particle impact damping: effect of mass ratio, material, and shape, J. Sound. Vib. (2005).
[35] M. Sanchez, M. Carlevaro, L.A. Pugnaloni, Effect of particle shape and fragmentation on the response of particle dampers, J. Vib. Control 20 (12) (2014) 1846–1854.
[36] L. Zheng, S.F. Masri, L. Xilin, Studies of the performance of particle dampers attached to a two-degrees-of-freedom system under random excitation, J. Vib. Control 17 (10) (2010) 1454–1471.
[37] K. Li, A.P. Darby, Experiments on the effect of an impact damper on a multiple-degree-of-freedom system, J. Vib. Control 12 (5) (2016) 445–464.
[38] E.-O. Stephen, I.C. Desen, Experimental study on an impact vibration absorber, J. Vib. Control (2001).
[39] A. Papalou, S.F. Masri, An experimental investigation of particle dampers under harmonic excitation, J. Vib. Control 4 (4) (1998) 361–379.
[40] N. Meyer, R. Seifried, Damping prediction of particle dampers for structures under forced vibration using effective fields, Granul. Matter. 23 (3) (2021).
[41] N. Meyer, R. Seifried, Toward a design methodology for particle dampers by analyzing their energy dissipation, Comput. Part Mech. 8 (4) (2020) 681–699.
[42] F.A.M. Galarza, et al., Design and experimental evaluation of an impact damper to be used in a slender end mill tool in the machining of hardened steel, Int. J. Adv. Manuf. Technol. 106 (5-6) (2019) 2553–2567.
[43] N. Popplewell, M. Liao, A simple design procedure for optimum impact dampers, J. Sound. Vib. (1991).
[44] M. Sánchez, G. Rosenthal, L.A. Pugnaloni, Universal response of optimal granular damping devices, J. Sound. Vib. 331 (20) (2012) 4389–4394.
[45] B.S. Wang, et al., Experimental and optimization analysis of a multiple unidirectional single-particle damper, J. Sound. Vib. 553 (2023) 117664.
[46] H. Safaeifar, A. Farshidianfar, Experimental and analytical investigation of impact dampers in free vibration reduction with coulomb friction, Noise Vib. Worldw. 53 (3) (2021) 91–103.
[47] X. Huang, X. Li, J. Wang, Optimal design of inerter-based nonpacked particle damper considering particle rolling, Earthq. Eng. Struct. Dyn. 50 (7) (2021) 1908–1930.
[48] T. Ehlers, et al., Design of particle dampers for additive manufacturing, Addit. Manuf. 38 (2021).
[49] N. Meyer, R. Seifried, Numerical and experimental investigations in the damping behavior of particle dampers attached to a vibrating structure, Comput. Struct. 238 (2020).
[50] H. Xu, et al., Vibration transmission and energy dissipation of roll controlled by particle damping absorber, Int. J. Mech. Sci. 249 (2023) 108264.
[51] Z. Lu, et al., Experimental studies of the effects of buffered particle dampers attached to a multi-degree-of-freedom system under dynamic loads, J. Sound. Vib. 331 (9) (2012) 2007–2022.
[52] K. Li, A.P. Darby, Modelling a buffered impact damper system using a spring-damper model of impact, Struct. Control Health Monit. 16 (3) (2009) 287–302.
[53] K. Li, A.P. Darby, A buffered impact damper for multi-degree-of-freedom structural control, Earthq. Eng. Struct. Dyn. 37 (13) (2008) 1491–1510.
[54] K. Li, A.P. Darby, An experimental investigation into the use of a buffered impact damper, J. Sound. Vib. 291 (3-5) (2006) 844–860.
[55] L. Kuinian, D. Antony, An experimental investigation into the use of a buffered impact damper, J. Sound. Vib. (2006).
[56] C.C. Liao, Y.C. Chung, C.H. Weng, A study on the energy dissipation mechanism of dynamic mechanical systems with particle dampers by using the novel energy method, Nonlinear Dyn. 111 (17) (2023) 15955–15980.
[57] X. Li, et al., Study on the damping effect of particle dampers considering different surface properties, Shock Vib. 2019 (1) (2019) 1–16.
[58] M.A. Akbar, W.O. Wong, E. Rustighi, Design optimization of a single-mass impact damper, J. Sound. Vib. 570 (2024) 118019.
[59] C.S. Song, et al., Analysis of vibration reduction performance of vibration isolation system based on particle damping, J. Low Freq. Noise Vib. Act. Control (2024).
[60] X. Li, et al., Irreversible energy transfers in systems with particle impact dampers, Nonlinear Dyn. 112 (1) (2024) 35–58.
[61] S. Kumar, A. Kumar, Vibration attenuation of a PCB enclosure in a radar system employing internal particle dampers, Int. J. Mech. Mater. Des. (2024).
[62] R.L. Jackson, I. Green, D.B. Marghitu, Predicting the coefficient of restitution of impacting elastic-perfectly plastic spheres, Nonlinear Dyn. 60 (3) (2009) 217–229.
[63] M.A. Akbar, W. Wong, E. Rustighi, A study of soft and hard impact effects in single-particle impact dampers, J. Vib. Control 0 (0) (2024) 10775463241273063.
[64] K.R.B. Melo, T.F. de Pádua, G.C. Lopes, A coefficient of restitution model for particle–surface collision of particles with a wide range of mechanical characteristics, Adv. Powder. Technol. 32 (12) (2021) 4723–4733.
[65] Q. Peng, et al., Effect of plasticity on the coefficient of restitution of an elastoplastic sphere impacting an elastic plate, Int. J. Solids. Struct. 222-223 (2021) 111036.
[66] Z. Li, Y. Du, Interval of restitution coefficient for chattering in impact damper, J. Low Freq. Noise Vib. Act. Control 41 (2) (2022) 432–450.
[67] G. Wang, C. Liu, Y. Liu, Energy dissipation analysis for elastoplastic contact and dynamic dashpot models, Int. J. Mech. Sci. 221 (2022) 107214.
[68] W.O. Wong, R.P. Fan, F. Cheng, Design optimization of a viscoelastic dynamic vibration absorber using a modified fixed-points theory, J. Acoust. Soc. Am. 143 (2) (2018) 1064–1075.
[69] K. Nering, A. Kowalska-Koczwara, Determination of vibroacoustic parameters of polyurethane mats for residential building purposes, Polymers 14 (2) (2022).

[70] D. Qiu, Y. He, Z. Yu, Investigation on compression mechanical properties of rigid polyurethane foam treated under random vibration condition: an experimental and numerical simulation study, Materials 12 (20) (2019).
[71] P.S. Patel, D.E. Shepherd, D.W. Hukins, Compressive properties of commercially available polyurethane foams as mechanical models for osteoporotic human cancellous bone, BMC Musculoskelet. Disord. 9 (1) (2008) 137.
[72] D.B. Hastie, Experimental measurement of the coefficient of restitution of irregular shaped particles impacting on horizontal surfaces, Chem. Eng. Sci. 101 (2013) 828–836.
[73] P.A. Hassan, G. Verma, R. Ganguly, Soft materials — Properties and applications, Funct. Mater. (2012) 1–59.
[74] M.S. Rajput, et al., Compression of structural foam materials – Experimental and numerical assessment of test procedure and specimen size effects, J. Sandw. Struct. Mater. 21 (1) (2017) 260–288.